Distant Galaxy Source Densities and Emission Line Fluxes

For Gemini/MCAO
Prepared by Chip Kobulnicky

The purpose of this document is to review the expected surface densities and luminosities of galaxies in the infrared wavebands that will drive the sensitivity and multi-object design requirements of MCAO and related instrumentation.

1.1: Surface Density of K-band Continuum Sources

Bershady, Lowenthal, & Koo (1998) measure K band luminosity functions and compile K-band luminosity functions from many authors (**Fig. 1-left**). The find 50 sources arcmin^{-2} with $K < 22$ ($\equiv$ AB(2.2 μm)=24 $\equiv$ 9.3×10^{-7} Jy). Fig. 1-right shows the expected galaxy surface density as a function of K-band continuum flux. The first dashed line at K(AB)=20.5 shows the limiting sensitivity for a 10σ detection in 4 hr with R=100 in the case of an extended galaxy with a uniform surface brightness over 1 arcsec^2. Clearly, there will be very few sufficiently-bright galaxies within the 1.5' diameter MCAO field-of-view to warrant more than 3-5 IFUs. Spectroscopic detections of continuum objects will be extremely difficult, although the situation improves as galaxies become more compact and approach point sources. The second dashed line illustrates the continuum sensitivity to point sources with a 0.10" IFU, taken from the Baldry & Taylor sensitivity simulations (see Appendix). In this most optimistic scenario, if *all* redshift ranges are included, and if all sources are point-like (clearly overly-optimistic), then there will be between 10 and 30 targets per armin^2 which are bright enough for 10σ continuum detections.

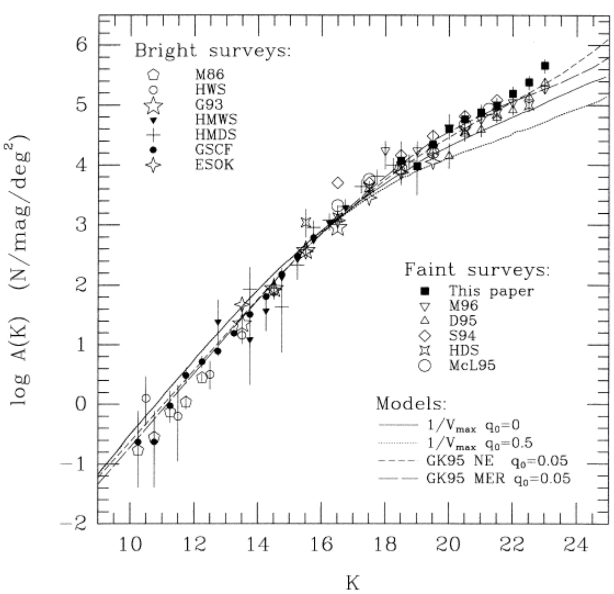

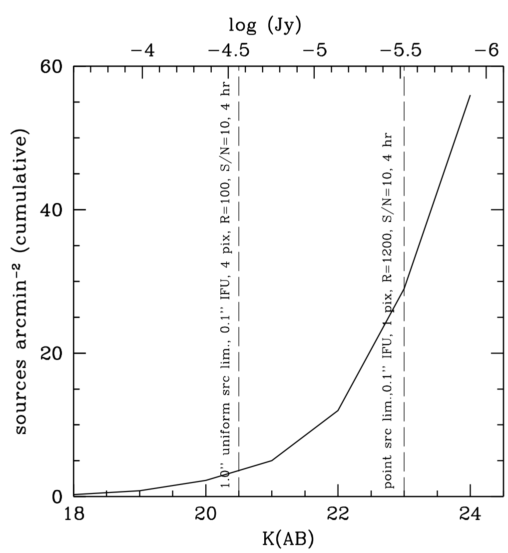

1.2: Surface Density of Continuum Sources as a Function of Redshift

If we consider sources as a function of redshift, we begin with the I band luminosity function and redshift distribution from the Hubble Deep Field North (Fernandez-Soto, Lanzetta, & Yahil 1999; **Fig. 2-left**) which can be used to estimate what fraction of these objects brighter than some fiducial magnitude, (say, I(AB)=26), will be in an interesting redshift range. From this figure it is clear that for targets brighter than I(AB)=26, the surface densities peak near 22 objects arcmin^{-2} per 0.4 z units occurs when z=0.5-1.5. This is the redshift range where having up to 30 IFUs may make sense, if a sufficiently high number fraction of these objects are above the detection threshold. Based upon the arguments in Section 1.1 above, spectroscopic continuum detections will be very difficult regardless of redshift, but spectroscopic detection of emission lines will be most common. **Fig. 2-right** shows the cumulative fraction of objects brighter than I(AB)=26 with redshifts $< z$ based on the HDF data. Only ∼30% of the objects have redshifts larger than 1 which would be required to place the strong optical emission lines in the infrared bandpasses. These estimates of galaxy number density are consistent with the findings of Adelberger et al. (1998) that the number of Lyman break galaxies with $< R = 25.5$ ($z \geq 3$) is ∼0.5 arcmin^{-2}.

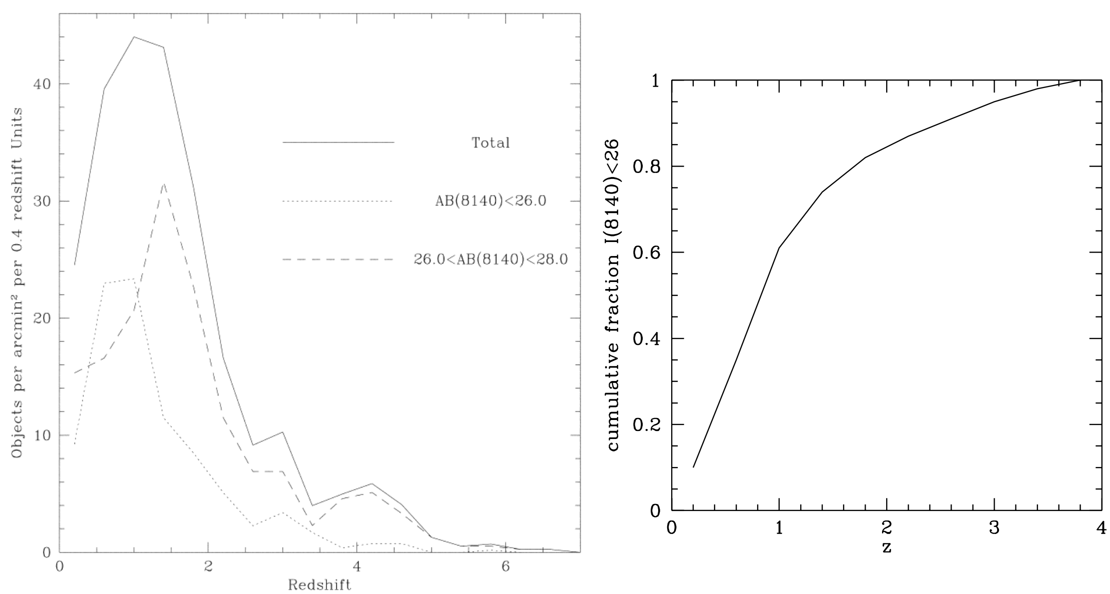

1.3: Surface Densities of Emission Line Sources

The EW for $H\alpha$ in local galaxies ranges from ∼30 in local spiral galaxies (Kennicutt 1992) to ∼1000 for some extreme HII galaxies and individual HII regions within larger galaxies. EWs are are further boosted by a factor 1+z for distant objects. We illustrate the range of expected emission line fluxes/magnitudes below. If we assume that Hα in a typical galaxy will have an observed EW=100 and a velocity width of 100 km/s FWHM (see Pettini et al. 1998, 2001 or Kobulnicky & Koo 2000 for the higher-redshift universe), or about 6.7 Å (1.5×10^8 Hz) in the observed frame at 2 μm, then we can use the K-band luminosity function from the above section to estimate their $H\alpha$ fluxes. (Recall that 1 Jy $= 1 \times 10^{-23}$ $erg\ s^{-1}\ cm\ Hz^{-1}$).

Table 1: Monochromatic Hα Magnitudes/Fluxes for Emission Lines

AB(2.2 μm) mag	Jy	EW(Hα) (Å)	AB(Hα) mag	Jy	F(Hα) ($erg/s/cm^2$)
20 (K=18)	3.6×10^{-5}	100	15	3.6×10^{-3}	1.8×10^{-15}
22 (K=20)	5.8×10^{-6}	100	17	5.8×10^{-4}	2.9×10^{-16}
24 (K=22)	9.3×10^{-7}	100	19	9.3×10^{-5}	4.6×10^{-17}

The detectability of emission lines will depend upon how many sub-apertures the flux is divided among, the sky conditions, and resolving power. See related document by Ivan Baldry & Taylor. Section 1.6 below, and observational evidence suggests that the sizes of emission line regions will be ~1-2 arcsec over a wide range of redshifts. However, the actual fraction of galaxies with emission lines larger than a given equivalent width is poorly known, and is likely to be highly dependant upon factors like redshift and local density. Nevertheless, some reasonable approximations can be made

Figure 3 shows the number of emission-line sources per arcmin^2 stronger than a given $H\alpha$ flux assuming that all the K-band sources from Figure 1 have EW(Hα)=200 (solid curve–clearly an overly-optimistic assumption), or EW(Hα)=20 (dotted curve). The vertical dashed lines show the limits of detectability (4 hrs integration, 10σ) for two different sky conditions. This figure shows that, under most sky conditions, between 5 and 30 emission line sources will be detectable in a given MCAO field *over all redshift ranges.* At redshifts beyond 1 where common strong nebular lines lie within the infrared bands, the number of detectable objects is likely to be 30% of this number. An exception might be special fields centered on known galaxies clusters (e.g., Pascarelle et al. 1996, 1998 on the field surrounding the z=2.4 radio galaxy 53W002). However, the Hα emission from most of these sub-galactic clumps at such redshifts ($F_{H\alpha} < 10^{-17}$ $erg\ s^{-1}\ cm^{-2}$) is beyond the detection limits of even 10 m class telescopes for reasonable integration times.

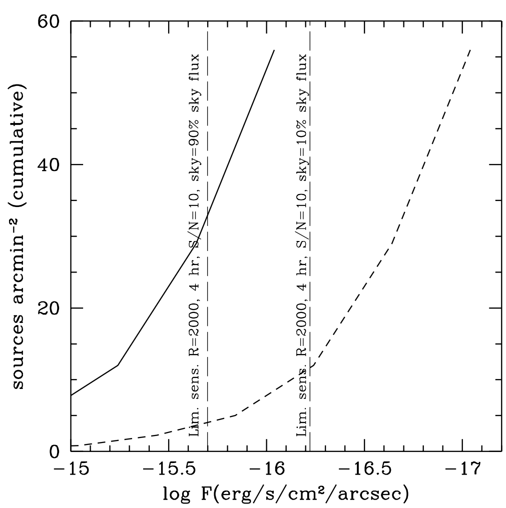

An observational check on the surface densities of emission-line objects comes from the narrowband imaging of Moorwood et al. (2000, A&A 362, 9) who find Hα emitters near $z = 2.2$ using a narrow band filter with $\Delta z = 0.03$. They find 10 objects in 100 arcmin^2 with typical $H\alpha$ fluxes of 1×10^{-16} $erg\ s^{-1}\ cm^2$. This is comparable to the K=24, EW=100 case in Table 1. If we assume that $H\alpha$ or the similarly strong [O III] λ5007 is visible in the IR continuously for redshifts $z = 1.0 - 3.0$ (total $\Delta z = 1.5$ allowing for redshift ranges inaccessible due to IR atmospheric opacity) then we expect about 5 such objects per arcmin^2, comparable to the previous estimates above.

1.4: Sizes of High-Redshift Galaxies

The detectability of distant galaxies will depend on the size, and thus, the surface brightness of the source. Figure 4 below shows the typical angular diameters for galaxies diameters of 2 kpc and 10 kpc as a function of redshift. The apparent source sizes for objects beyond z$\sim$1 are nearly constant, and will range between 0.3 and 1.2 arcsec.

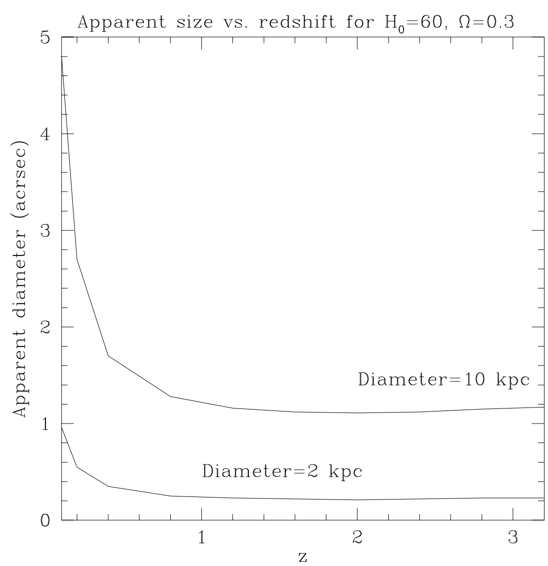

This figure implies that IFUs with 12x12 0.1$''$ apertures should be sufficient to cover typical objects at high redshifts. The 0.1$''$ apertures will provide a minimum of 3 spatial resolution elements across the smallest objects.

1.5: Surface Density of Galaxies in Intermediate Redshift Clusters

I take, as an example, the z=0.83 cluster, MS1054-03 (van Dokkum et al. 2000). They spectroscopically identify 78 cluster members with $I < 22$ in a 5'x7' region. Assuming this cluster's size is typical for intermediate redshifts, then the mean surface density is 3-4 objects arcmin^{-2} with $I < 22$ once their completeness corrections are applied. If a typical I-K color of an emission line galaxy is ~ 0.5, then we can pick up a few additional objects down to the nominal K=22 limits derived above for a total of ~ 6 objects with $K < 22$ arcmin^{-2}. Of these, only 35% of the von Dokkum et al. sample have emission lines. That would leave 2-3 emission line objects arcmin^{-2} in a given cluster. Within the 1.5' diameter field of MCAO, $\sim 6-9$ galaxies brighter than $K = 22$ (5×10^{-17} erg s^{-1} cm^{-2}) would be observable in emission lines.